Submitted to the
XXII International Symposium on Lepton-Photon Interactions at High Energy
30 June - 5 July, Uppsala, Sweden

Abstract: 293 **Session: QCD/HS**

Diffractive photoproduction of dijets at HERA

ZEUS Collaboration

Abstract

The diffractive photoproduction of dijets has been studied using $77.6\,\mathrm{pb}^{-1}$ of data taken by the ZEUS detector at HERA. The measurements have been made in the kinematic range $0.2 < y < 0.85$ and $x_{I\!P} < 0.025$, where y is the inelasticity and $x_{I\!P}$ is the fraction of the proton momentum taken by the diffractive exchange. The jets are reconstructed using the longitudinally invariant k_T algorithm and the two highest transverse energy jets are required to satisfy $E_T > 7.5$ and $6.5\,\mathrm{GeV}$, respectively. Both jets are required to lie in the pseudorapidity range $-1.5 < \eta < 1.5$. Double differential cross sections have been measured for direct and resolved enriched photoproduction and are confronted with the predictions from leading-logarithm parton-shower Monte Carlo models and next-to-leading-order QCD calculations, which use the diffractive parton distribution functions extracted from QCD DGLAP fits to inclusive diffractive deep inelastic scattering measurements.

1 Introduction

An important question which arises in hard diffractive processes is whether they can be factorized into universal diffractive parton distribution functions (PDFs) and the partonic cross section. The QCD factorization theorem has been proven to be valid for diffractive deep inelastic scattering (DIS) [1, 2]. This implies that diffractive parton distributions can be defined for the proton, and their evolution predicted using the DGLAP evolution equations, as with the usual inclusive PDFs. At HERA, the diffractive PDFs have been extracted from QCD DGLAP fits to inclusive diffractive DIS data [3–5]. As a test of factorization, the extracted PDFs can be used for the calculation of exclusive processes with different hadronic final states.

Recent measurements of dijet and D^* production by the ZEUS and H1 Collaborations have supported the factorization theorem in diffractive DIS [6, 7], as predicted theoretically. Factorization is not expected to work in $\bar{p}p$ diffractive hard interactions, where rescattering processes between the two hadron beams are predicted [8]. Such rescattering processes create additional particles that fill the large rapidity gap characteristic of diffractive scattering events and thus determine a suppression of the data. One such rescattering model predicts that the resolved photoproduction is suppressed by a factor 0.34 [9].

The factorization theorem and such rescattering models can be tested in diffractive photoproduction in both direct and resolved processes [10, 11]. Direct photon processes are viewed to be similar as DIS, since the photon is point-like and factorization is expected to hold. However, in resolved photon processes, the photon acts as a source of partons, with only a fraction of its momentum participating in the hard scatter. In this case rescattering is expected between the hadron-like exchanged photon and the proton. Experimentally, the two processes are distinguished from one another by x_γ^{obs}, the longitudinal momentum fraction of the photon taken by the dijet system. The ranges x_γ^{obs} greater than 0.75 and less than 0.75 correspond to regions enriched with direct and resolved photon processes, respectively.

This paper presents measurements of the diffractive photoproduction of dijets made using the ZEUS detector at HERA. A 30-fold increase in luminosity has been achieved compared to the previous ZEUS analysis [12], which in combination with the addition of a new forward[1] detector, allows precise measurements to be made in a wider kinematic range. Measured differential cross sections are compared to Monte Carlo (MC) models

[1] The ZEUS coordinate system is a right-handed Cartesian system, with the Z axis pointing in the proton beam direction, referred to as the "forward direction", and the X axis pointing left towards the center of HERA. The coordinate origin is at the nominal interaction point.

and next-to-leading-order (NLO) predictions which use the diffractive PDFs extracted from inclusive diffractive DIS measurements [3, 4].

In this analysis comparisons between data and theoretical predictions are made for kinematic ranges enriched in direct and resolved processes.

2 Experimental set-up

This analysis uses an integrated luminosity of $77.6\,\text{pb}^{-1}$ collected with the ZEUS detector [13] at the HERA collider during the $1999-2000$ data-taking period. The incoming positron[2] and proton energies were 27.5 and 920 GeV, respectively. The jets are reconstructed using the central tracking detector (CTD) [14] and uranium-scintillator calorimeter (CAL) [15]. Diffractive events are selected by requiring a large rapidity gap in the forward calorimeter (FCAL) and the forward plug calorimeter (FPC) [16], which was placed inside the FCAL, close to the beam pipe.

3 Kinematics and data selection

In this analysis, diffractive dijet photoproduction processes ($ep \to ep + X(\text{jet} + \text{jet} + X'))$ are defined by a final state consisting of a scattered positron and a scattered proton, both of which escape down the beam pipe, and a hadronic system X, with invariant mass M_X, which contains the dijet system from the hard scattering. The kinematic variables describing this process are defined as follows:

- y, the fraction of the positron energy carried by the photon in the proton rest frame;
- Q^2, the photon virtuality;
- $x_{I\!P}$, the momentum fraction lost by the proton;
- $E_T^{\text{jet1,2}}$ and $\eta^{\text{jet1,2}}$, transverse energy and pseudorapidity, respectively, of the two highest E_T jets reconstructed by the k_T algorithm [17], which is run in the longitudinally invariant inclusive mode [18] in the laboratory frame.

The kinematic variables and jets are reconstructed from energy flow objects (EFOs) which combine energy clusters reconstructed in the CAL and charged tracks reconstructed in the CTD [19]. In particular, M_X is reconstructed as $M_X = \sqrt{\sum(E-p_z)\cdot\sum(E+p_z)}$, where the sum runs over all EFOs. EFOs are additionally corrected for energy losses due

[2] Hereafter, “positron” is used to refer to both electron and positron beams.

to dead material in front of the CAL. The reconstructed values correspond well to their true values with good resolution, based on Monte Carlo studies.

The cross sections are measured in the following kinematic region:

- $0.2 < y < 0.85$, $Q^2 < 1\,\mathrm{GeV}^2$;
- $x_{I\!P} < 0.025$;
- $E_T^{\mathrm{jet1}} > 7.5\,\mathrm{GeV}$, $E_T^{\mathrm{jet2}} > 6.5\,\mathrm{GeV}$, $-1.5 < \eta^{\mathrm{jet1,2}} < 1.5$.

Photoproduction events are selected by requiring that no scattered positron candidate is identified. Diffractive events are selected by requiring a large rapidity gap which covers the pseudorapidity range $3 < \eta < 5$, where $\eta \approx 5$ corresponds to the forward edge of the FPC. After applying these selection requirements, an additional 2% of the events are rejected as background from cosmic events based on the timing of the two highest E_T jets. Furthermore, the background from proton dissociation events, with a low-mass proton dissociative system escaping down the beam pipe, is estimated to be (16±4)% [6] and is subtracted from all measured cross sections. The proton-dissociative background is checked to be independent of all the kinematic variables used to quote the cross sections. The contribution from non-diffractive background events is estimated to be small (5%) from the Pythia MC programme [20]. This is not subtracted. A total of 7411 events remain after all selection cuts.

Two additional variables are used in this analysis:

$$z_{I\!P}^{obs} = \frac{\sum_{jets} E_T^{\mathrm{jet}} e^{\eta^{\mathrm{jet}}}}{2x_{I\!P}E_p} \qquad x_{\gamma}^{obs} = \frac{\sum_{jets} E_T^{\mathrm{jet}} e^{-\eta^{\mathrm{jet}}}}{2yE_e} \tag{1}$$

where the sums run over the two highest E_T jets. The observable $z_{I\!P}^{obs}$ (x_{γ}^{obs}) is an estimator of the longitudinal fractional momentum taken from the diffractive exchange (photon) by the dijet system produced in the hard scattering. The observable $z_{I\!P}^{obs}$ is sensitive to the parton densities in the diffractive exchange, while the ranges x_{γ}^{obs} greater than 0.75 and less than 0.75 correspond to regions enriched with direct and resolved photon processes, respectively.

4 Theoretical predictions

Data are compared to both LO and NLO predictions at the hadron level (i.e. level of stable hadrons).

The LO predictions are made using the Rapgap Monte Carlo generator [21] interfaced to the parton shower model Meps [22], and the hadronization model Jetset [20]. The diffractive PDFs determined by the H1 Collaboration (H1 fit 2) [3] and the photon structure function GRV-G-HO [23] are used. This Monte Carlo generator is also used to correct the data to the hadron level.

Two sets of NLO QCD calculations are compared to the data: a model with the resolved photon suppressed by a factor of R=0.34 and a model with no suppression (R=1) [24]. The results of the recent preliminary NLO QCD fits made by the H1 Collaboration (H1 2002 fit (prel.)) are used for the diffractive parton densities [4]. The parton level predictions are corrected to the hadron level using correction factors determined with RAPGAP. The extracted corrections are ~ 1.

5 Results

Double differential cross sections for direct enriched ($x_\gamma^{obs} > 0.75$) and resolved enriched ($x_\gamma^{obs} < 0.75$) photoproduction and the ratio of the two ($\sigma(x_\gamma^{obs} < 0.75)/\sigma(x_\gamma^{obs} > 0.75)$ are measured as functions of y, $x_{I\!P}$, M_X, $z_{I\!P}^{obs}$, $E_T^{\rm jet1}$ and $\eta^{\rm jet1}$.

Predictions from the RAPGAP MC, which use the H1 Fit 2 diffractive PDFs [3], are normalized to the data by a global factor of 0.53. Apart from $z_{I\!P}^{obs}$, which is sensitive to the uncertainties of the diffractive gluon distributions, the RAPGAP MC gives a good description of the shapes of all variables for both the direct and resolved enriched samples, as shown in Figs.1 and 2, respectively.

The ratio of the resolved enriched to the direct enriched cross section as a function of y, $x_{I\!P}$, M_X, $z_{I\!P}^{obs}$, $E_T^{\rm jet1}$ and $\eta^{\rm jet1}$ is shown in Fig.3 and compared to the RAPGAP MC. Taking the cross section ratio cancels uncertainties such as those due to the diffractive PDFs, providing a more reliable comparison with the predictions. The ratios are well described as a function of all variables, indicating that the RAPGAP MC reproduces both the direct and resolved enriched samples alike in various kinematic regions. A suppression of the resolved photoproduction data is expected to be observed from certain theoretical calculations (e.g. [9]), but no such evidence is found. Overall, both direct and resolved photoproduction data are well described by the RAPGAP MC.

The NLO QCD calculations after hadronization correction are compared to the data in Figs.4 and 6 for samples enriched in direct and resolved processes, respectively. For $x_\gamma^{obs} > 0.75$, the NLO prediction gives a good description of the shape of the measured cross sections, although it lies a factor of two above in absolute normalisation (Fig.5). For $x_\gamma^{obs} < 0.75$, the NLO calculation lies similary above the data in normalisation when no suppression (R=1) is applied (Fig.7) and below the data by a factor of two when a suppression, R=0.34, is applied to resolved photon processes. The general trends of the data for low x_γ^{obs} are reproduced by the NLO prediction. Some discrepancies are seen however in the y and η^{jet1} cross sections. Data at low x_γ^{obs} are also sensitive to the parametrization of the photon PDFs, the uncertainties of which are not evaluated here. A different photon PDF may improve the description of the data.

The ratio of the resolved enriched to the direct enriched is fairly well reproduced by NLO predictions with R=1 (Fig.8), indicating that a suppression of the resolved data with respect to the direct is not observed in any particular kinematic region.

In summary, no evidence is observed for a suppression of resolved photon processes relative to direct photon processes in diffractive dijet photoproduction. A uniform suppression for both resolved and direct processes gives a better description of the data, however the uncertainties in the diffractive PDFs need to be evaluated before stronger conclusions can be made.

Acknowledgments

We would like to thank M. Klasen and G. Kramer for providing the NLO predictions. We are grateful to the H1 Collaboration for allowing us the use of the H1 fit 2002 (prel.).

References

[1] J.C. Collins, Phys. Rev. **D 57**, 3051 (1998).

[2] L. Trentadue and G. Veneziano, Phys. Lett. **B 323**, 201 (1994).

[3] H1 Coll., C. Adloff et al., Z. Phys. **C 76**, 613 (1997).

[4] H1 Coll., *paper 980 submitted to 31. Intl. Conf. on High Energy Physics ICHEP 2002, Amsterdam, and paper 089 submitted to the EPS 2003 Conf., Aachen* (unpublished).

[5] ZEUS Coll., S. Chekanov et al., Eur. Phys. J. **C 38**, 43 (2004).

[6] ZEUS Coll., S. Chekanov et al., Nucl. Phys. **B 672**, 3 (2003).

[7] H1 Coll., C. Adloff et al., Eur. Phys. J. **C 20**, 29 (2001).

[8] A.B. Kaidalov et al., Eur. Phys. J. **C 21**, 521 (2001).

[9] A.B. Kaidalov et al., Phys. Lett. **B 567**, 61 (2003).

[10] ZEUS Coll.. Paper 249 submitted to the *32nd International Conference on High Energy Physics ICHEP 2004*, Beijing, China, available on `http://www-zeus.desy.de/physics/phch/conf/ichep04/index.html`.

[11] H1 Coll.. Paper 177 submitted to the *32nd International Conference on High Energy Physics ICHEP 2004*, Beijing, China, available on `http://www-h1.desy.de/h1/www/publications/conf/conf_list.html`.

[12] ZEUS Coll., J. Breitweg et al., Eur. Phys. J. **C 5**, 41 (1998).

[13] ZEUS Coll., U. Holm (ed.), *The ZEUS Detector*. Status Report (unpublished), DESY (1993), available on `http://www-zeus.desy.de/bluebook/bluebook.html`.

[14] N. Harnew et al., Nucl. Inst. Meth. **A 279**, 290 (1989);
B. Foster et al., Nucl. Phys. Proc. Suppl. **B 32**, 181 (1993);
B. Foster et al., Nucl. Inst. Meth. **A 338**, 254 (1994).

[15] M. Derrick et al., Nucl. Inst. Meth. **A 309**, 77 (1991);
A. Andresen et al., Nucl. Inst. Meth. **A 309**, 101 (1991);
A. Caldwell et al., Nucl. Inst. Meth. **A 321**, 356 (1992);
A. Bernstein et al., Nucl. Inst. Meth. **A 336**, 23 (1993).

[16] ZEUS Coll., FPC group, A. Bamberger et al., Nucl. Inst. Meth. **A 450**, 235 (2000).

[17] S.Catani et al., Nucl. Phys. **B406**, 187 (1993).

[18] S.D. Ellis and D.E. Soper, Phys. Rev. **D 48**, 3160 (1993).

[19] G.M. Briskin, *Diffractive Dissociation in ep Deep Inelastic Scattering*. Ph.D. Thesis, Tel Aviv University, 1998. (Unpublished).

[20] M. Bengtsson and T. Sjöstrand, Comp. Phys. Comm. **46**, 43 (1987); T. Sjöstrand, Comp. Phys. Comm. **82**, 74 (1994).

[21] H. Jung, *The RAPGAP Monte Carlo for Deep Inelastic Scattering version 2.08/00* (unpublished). 2001.

[22] M. Bengtsson and T. Sjöstrand, Z. Phys. **C 37**, 465 (1998).

[23] M. Glück, E. Reya and A. Vogt, Z. Phys. **C 53**, 127 (1992).

[24] M. Klasen and G. Kramer, Eur. Phys. J. **C 38**, 93 (2004).

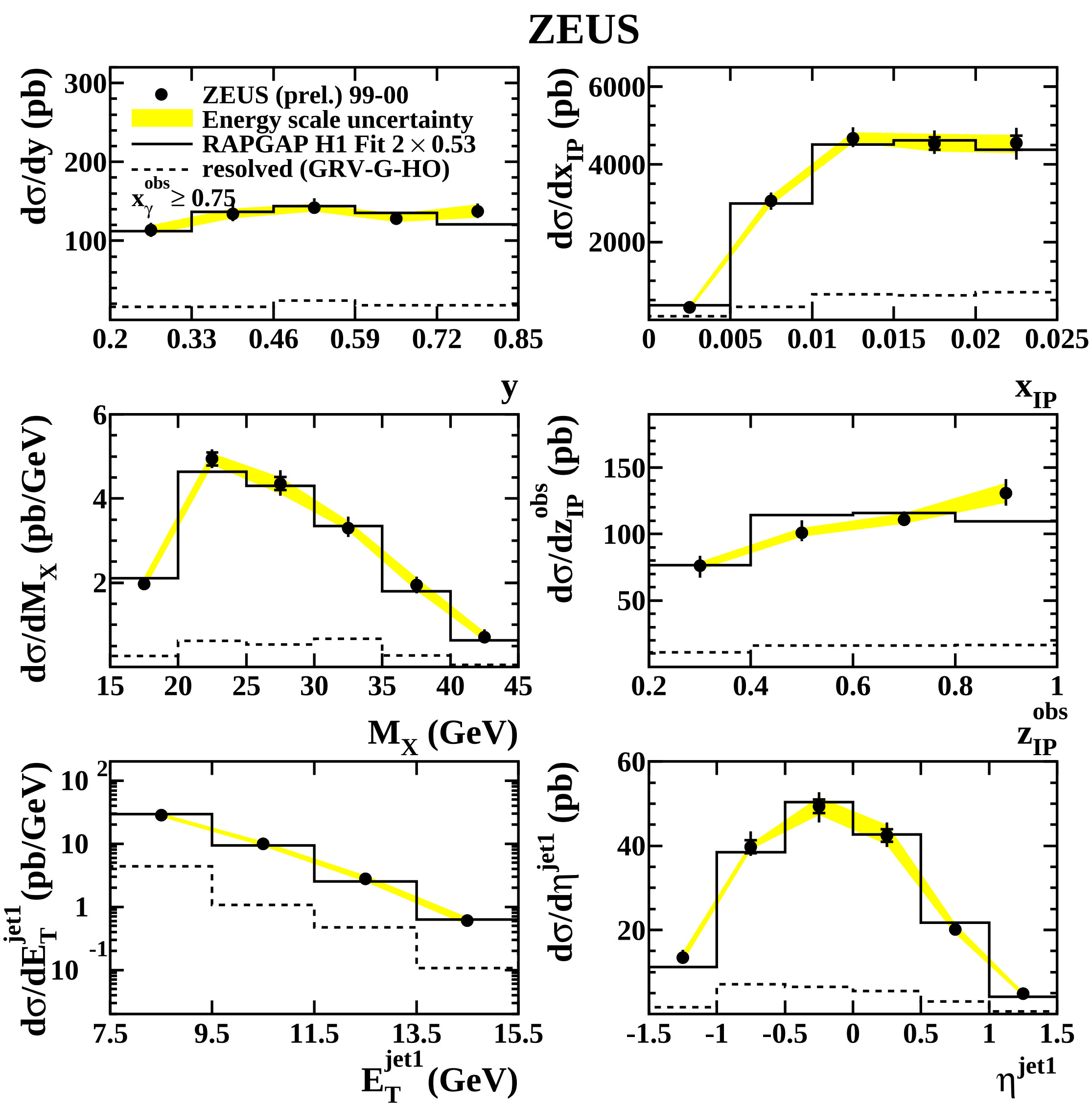

Figure 1: *The double differential cross sections for direct enriched photoproduction ($x_\gamma^{obs} > 0.75$) in y, $x_{I\!P}$, M_X, $z_{I\!P}^{obs}$, E_T^{rmjet1} and $\eta^{\rm jet1}$. The data are shown as dots, with the corresponding energy scale uncertainty shown as a band; the inner error bars indicate the statistical uncertainty and the outer error bars indicate the statistical and systematic uncertainties added in quadrature. The solid lines show the prediction of the LO* Rapgap *Monte Carlo, normalized to the data by a factor of 0.53; the dashed lines are the resolved photon component from* Rapgap. *The H1 Fit 2 diffractive PDFs are used [3].*

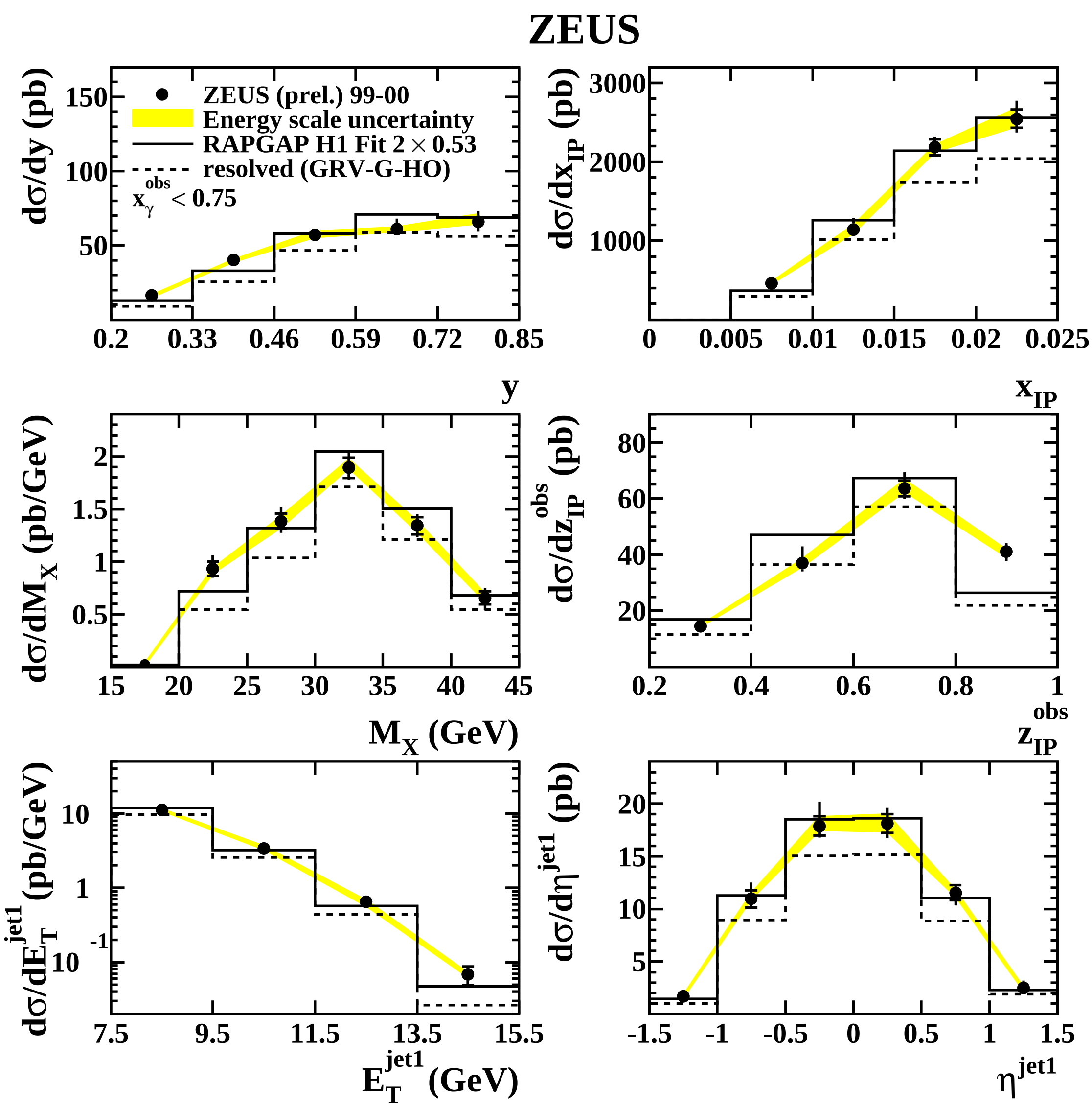

Figure 2: *The double differential cross sections for resolved enriched photoproduction ($x_\gamma^{obs} < 0.75$) in y, $x_{I\!P}$, M_X, $z_{I\!P}^{obs}$, $E_T^{\rm jet1}$ and $\eta^{\rm jet1}$. The data are shown as dots, with the corresponding energy scale uncertainty shown as a band; the inner error bars indicate the statistical uncertainty and the outer error bars indicate the statistical and systematic uncertainties added in quadrature. The solid lines show the prediction of the LO* Rapgap *Monte Carlo, normalized to the data by a factor of 0.53; the dashed lines are the resolved photon component from* Rapgap. *The H1 Fit 2 diffractive PDFs are used [3].*

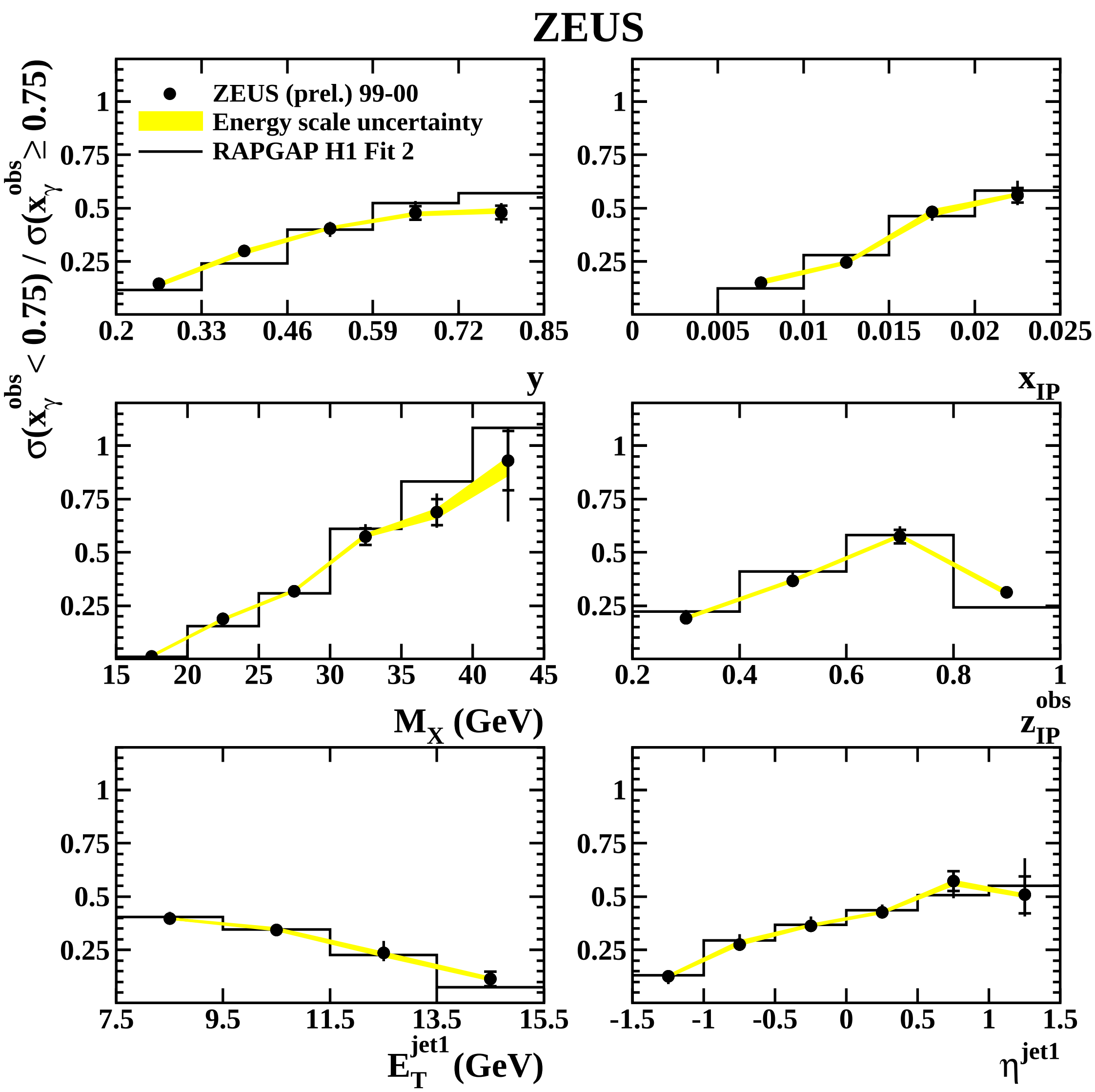

Figure 3: *The ratio of the double differential cross section with $x_\gamma^{obs} < 0.75$ to the double differential cross section with $x_\gamma^{obs} \geq 0.75$, as a function of y, $x_{I\!P}$, M_X, $z_{I\!P}^{obs}$, $E_T^{\rm jet1}$ and $\eta^{\rm jet1}$ for data (dots) and LO Monte Carlo prediction (solid lines). See the caption of Fig. 1 for a description of the data.*

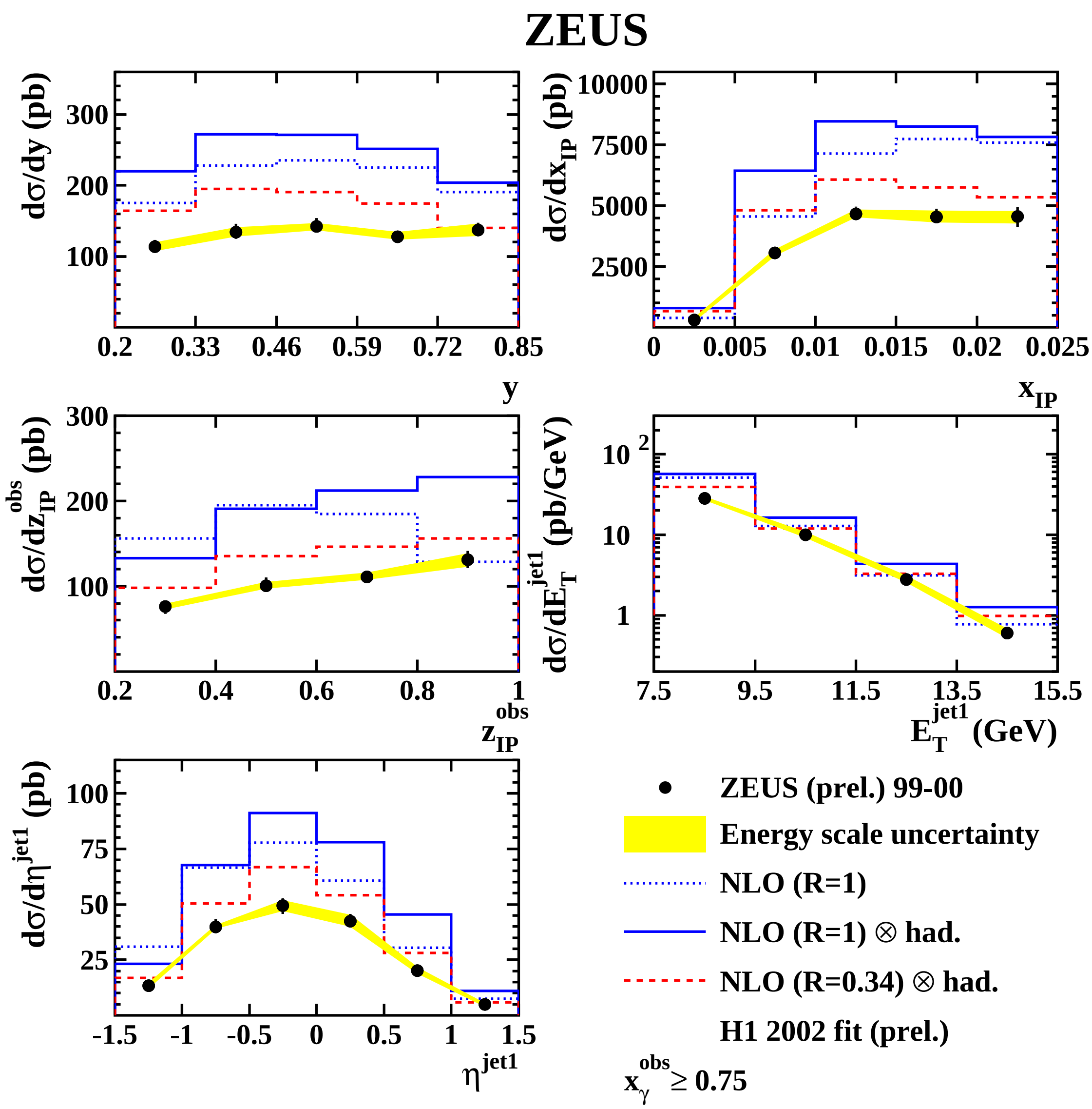

Figure 4: *The double differential cross sections for direct enriched photoproduction ($x_\gamma^{obs} > 0.75$) in y, $x_{I\!P}$, $z_{I\!P}^{obs}$, $E_T^{\rm jet1}$ and $\eta^{\rm jet1}$, compared to NLO QCD predictions. For details of the data, see the caption of Fig. 1. The prediction without resolved photon suppression (R=1) and its theoretical uncertainty is shown as the solid lines with the shaded band; the corresponding parton level prediction before hadronization correction is shown as the dotted lines. The prediction with a suppression factor of 0.34 on the resolved photon processes (R=0.34) is shown as the dashed lines. The diffractive PDFs are from the H1 2002 fit [3].*

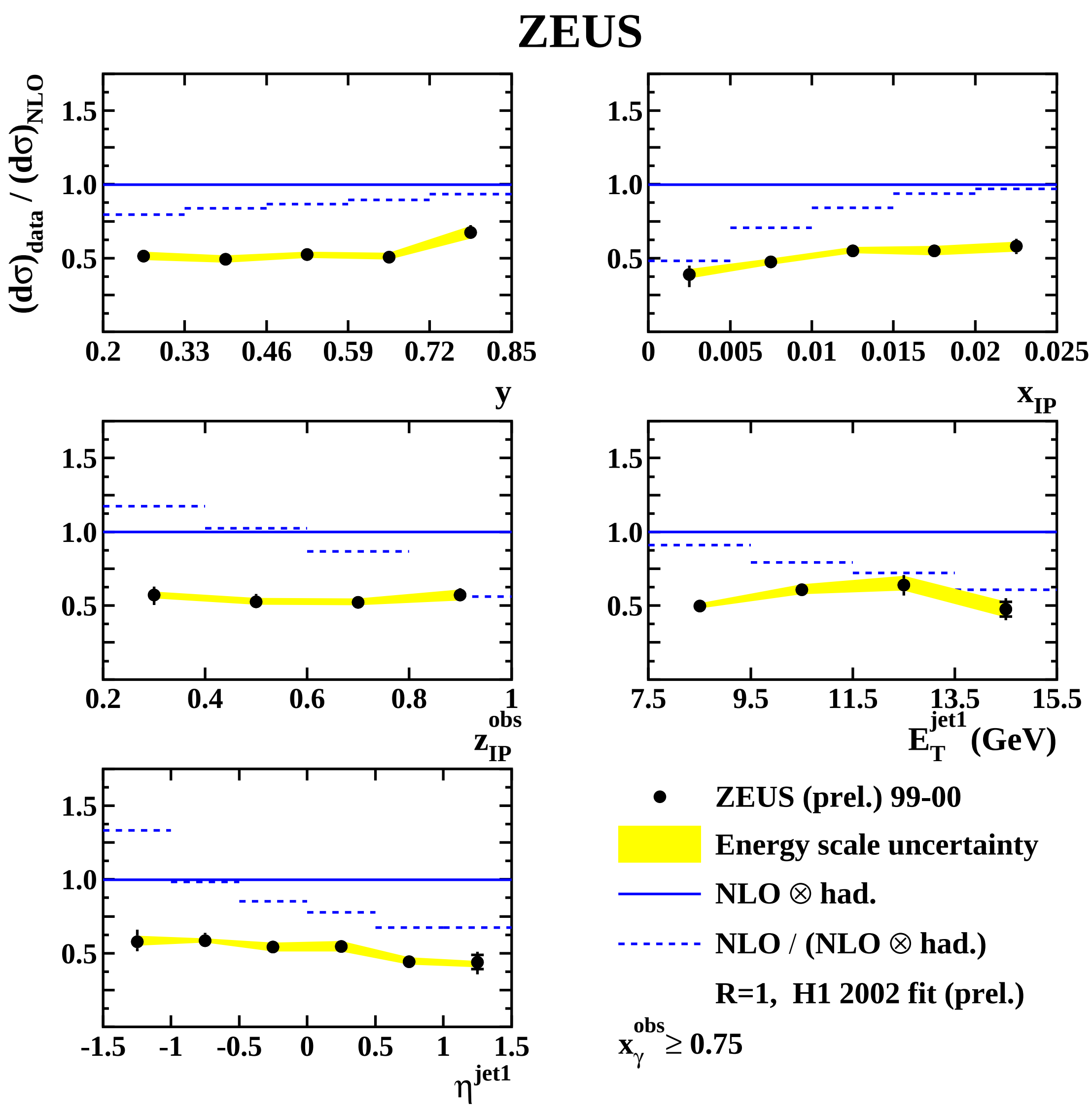

Figure 5: *The ratio of the double differential cross section with $x_\gamma^{obs} > 0.75$ in y, $x_{I\!P}$, $z_{I\!P}^{obs}$, $E_T^{\rm jet1}$ and $\eta^{\rm jet1}$, between data and NLO, for the prediction without resolved photon suppression (R=1). See the caption of Fig. 1 for the description of the data. The solid lines indicate the predictions; the dashed lines show the inverse of the hadronization correction factors, which are defined as the number of events selected at hadron level divided by the number of events selected at parton level. They are calculated with* RAPGAP.

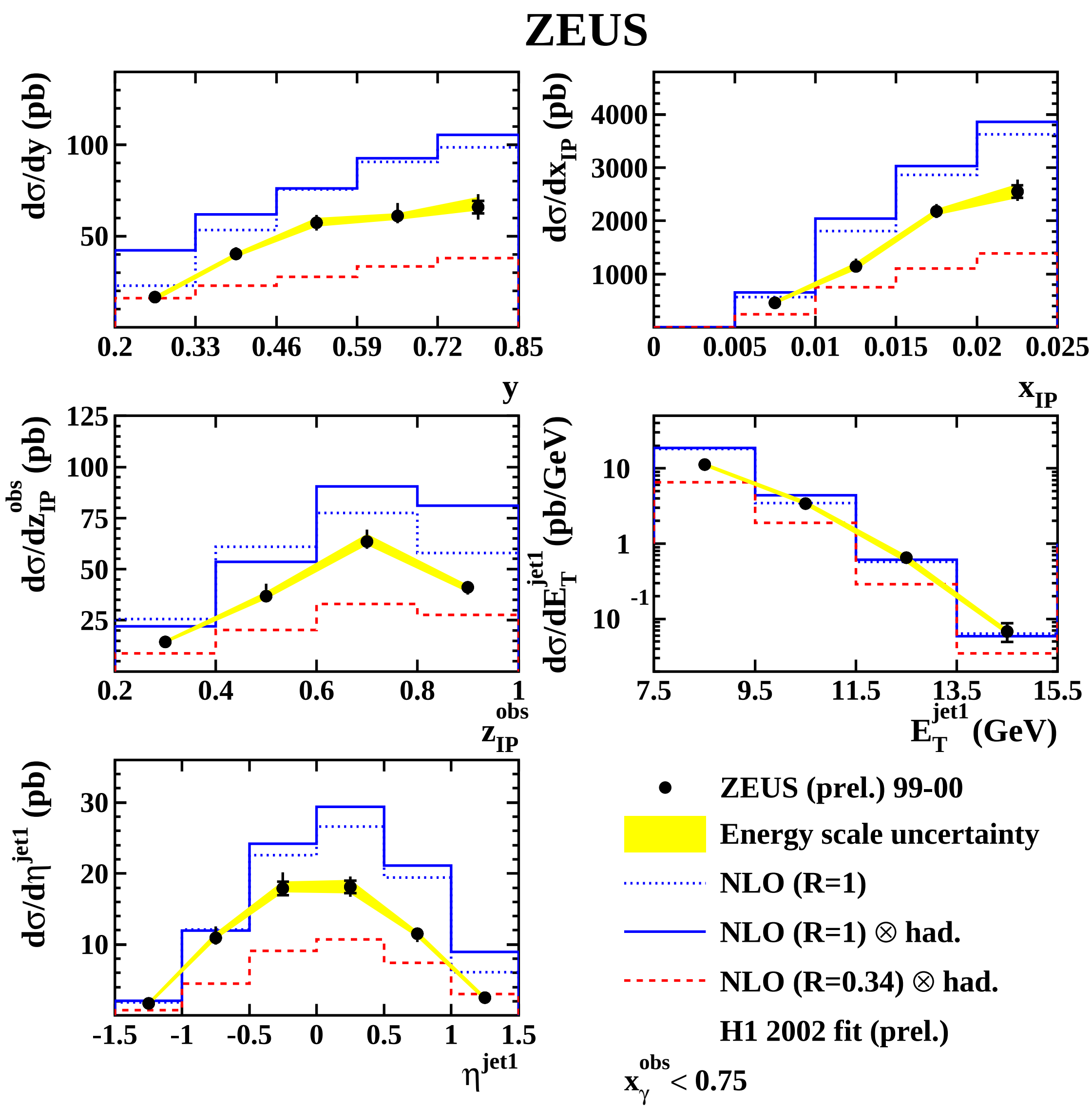

Figure 6: *The double differential cross sections for resolved enriched photoproduction ($x_\gamma^{obs} < 0.75$) in y, $x_{I\!P}$, $z_{I\!P}^{obs}$, $E_T^{\rm jet1}$ and $\eta^{\rm jet1}$, compared to NLO QCD predictions. For details of the data, see the caption of Fig. 1. The prediction without resolved photon suppression (R=1) and its theoretical uncertainty is shown as the solid lines with the shaded band; the corresponding parton level prediction before hadronization correction is shown as the dotted lines. The prediction with a suppression factor of 0.34 on the resolved photon processes (R=0.34) is shown as the dashed lines. The diffractive PDFs are from the H1 2002 fit [3].*

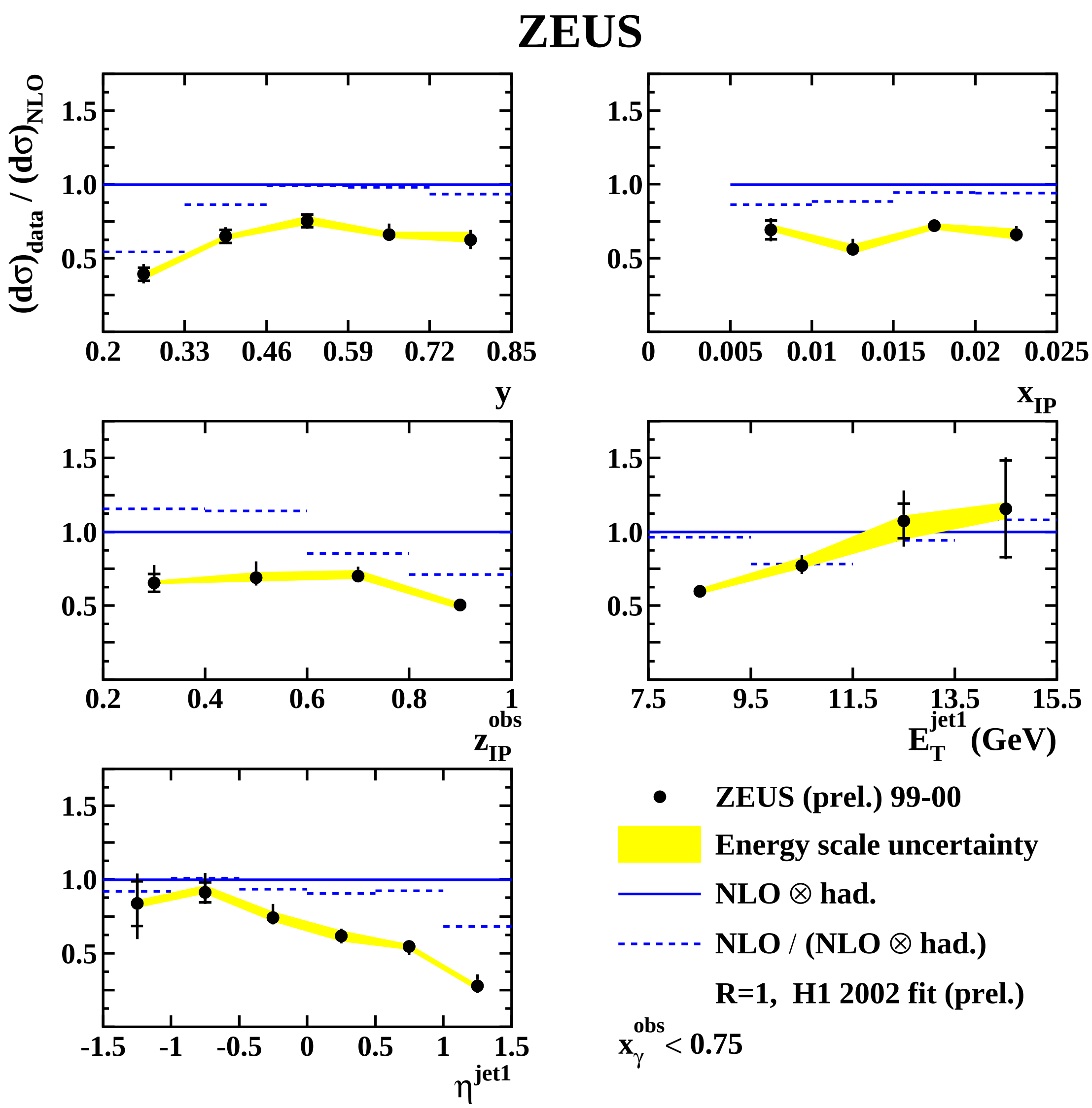

Figure 7: *The ratio of the double differential cross section with $x_\gamma^{obs} < 0.75$ in y, $x_{I\!P}$, $z_{I\!P}^{obs}$, $E_T^{\rm jet1}$ and $\eta^{\rm jet1}$, between data and NLO, for the prediction without resolved photon suppression (R=1). See the caption of Fig. 1 for the description of the data. The solid lines indicate the predictions; the dashed lines show the inverse of the hadronization correction factors, which are defined as the number of events selected at hadron level divided by the number of events selected at parton level. They are calculated with* RAPGAP.

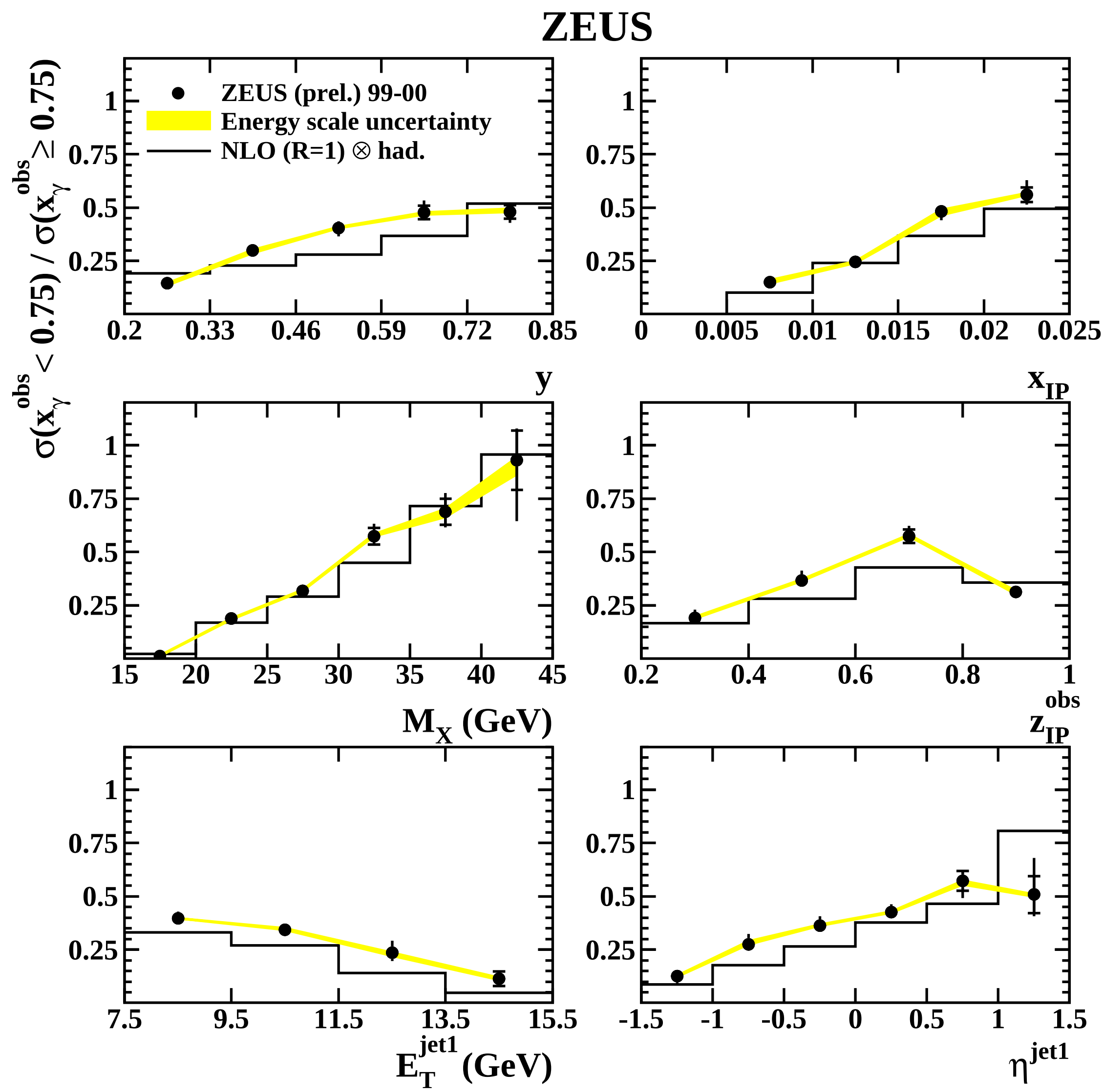

Figure 8: *The ratio of the resolved to the direct enriched differential cross section in y, $x_{I\!P}$, M_X, $z_{I\!P}^{obs}$, $E_T^{\rm jet1}$ and $\eta^{\rm jet1}$ compared to NLO predictions without resolved photon suppression (R=1). For a description of the data refer to Fig. 1.*